Wireless Power Transfer

cambridge.org/wptcup

Convex optimization of coil spacing in cascaded multi-coil wireless power transfer

Connor Badowich, Jacques Rousseau and Loïc Markley

School of Engineering, University of British Columbia, Kelowna, BC, V1V 1V7, Canada

Research Article

Cite this article: Badowich C, Rousseau J, Markley L (2020). Convex optimization of coil spacing in cascaded multi-coil wireless power transfer. *Wireless Power Transfer* **7**, 42–50. https://doi.org/10.1017/wpt.2020.5

Received: 19 August 2019
Revised: 29 November 2019
Accepted: 14 January 2020
First published online: 19 February 2020

Key words:
Cascaded resonators; convex optimization; magnetic resonance coupling; maximum efficiency; multi-coil system

Author for correspondence:
Loïc Markley, School of Engineering, University of British Columbia, Kelowna, BC, V1V 1V7, Canada.
E-mail: loic.markley@ubc.ca

Abstract

In this paper, we use convex optimization to maximize power efficiency through cascaded multi-coil wireless power transfer systems and investigate the resulting characteristic spacing. We show that although the efficiency is generally a non-convex function of the coil spacing, it can be approximated by a convex function when the effects of higher-order couplings are small. We present a method to optimize the spacing of cascaded coils for maximum efficiency by perturbing the solution of the convex approximation to account for higher-order interactions. The method relies on two consecutive applications of a local optimization algorithm in order to enable fast convergence to the global optimum. We present the optimal configurations of coil systems containing up to 20 identical coils that transfer power over distances up to 4.0 m. We show that when spacing alone is optimized, there exist an optimal number of coils that maximize transfer efficiency across a given distance. We also demonstrate the use of this method in optimizing the placement of a select number of high-Q coils within a system of low-Q relay coils, with the highest efficiencies occurring when the high-Q coils are placed on either side of the largest gaps within the relay coil chain.

Introduction

Wireless power transfer (WPT) technology has progressed rapidly in the past decade, with applications in mobile devices [1], electric vehicles [2], and medical implants [3, 4]. Many of these applications rely on magnetic resonance coupling (MRC) as the mechanism for power transfer, which uses inductive coils to transmit power across empty space [5, 6]. This technique offers many benefits including high efficiency at distances on the order of the radius of the coils, and low interaction with non-ferrous materials in surrounding environments. In recent years, applications with multiple transmitters distributed across large physical spaces have been introduced, such as charging electric vehicles while they are in-motion along a roadway [7], powering industrial machines in factories [8], and powering wireless sensor networks [9]. These new applications allow the receiver to be powered anywhere within the WPT environment, enabling greater mobility than in simple four-coil systems.

To improve the efficiency of WPT systems across greater distances, additional relay coils between a source and a load have been introduced and their effect on efficiency analyzed. Placing a single relay coil between a source and load has been shown to improve the efficiency of power transfer to the load, and it was shown that there exists an optimal location to place the relay coil for the greatest improvement to the efficiency [10, 11]. The analysis of relay coil systems and their effect on efficiency has also been extended to increasing numbers of relays [10–12], and to configurations of curved chains [10, 12, 13]. While many relay coil systems include a single electrical load, systems with a single transmitter coil and a load connected to each relay coil have also been analyzed [9, 14].

Optimization techniques have been applied to the design of multi-coil WPT systems containing many degrees of freedom. The spacing of cascaded chains of up to eight coils has been subject to optimization for maximum efficiency, while also solving for the optimal load resistance [10, 15]. It has been found that systems containing more than three coils have greater efficiency when the spacing between coils is unequal. Investigations into large multi-element systems with pre-determined fixed spacing have applied convex optimization techniques to determine the optimal reactive loading on each coil for maximum efficiency [16, 17]. In these works, convex optimization has been shown to provide a computationally efficient way to optimize the loading on cascaded chains of up to 12 coils and metamaterial arrays with up to 225 elements [17].

Here, we use convex optimization to find the optimal spacing in multi-coil cascaded resonator systems by showing that loosely coupled systems with high-quality factor coils can be modeled as perturbed convex systems. By optimizing the spacing of multi-coil systems, high-power transfer can be achieved without the need for individualized reactive tuning. This provides an alternative approach to the design of WPT systems that enables the use of

CAMBRIDGE UNIVERSITY PRESS

sets of identical coils. An expression for efficiency is generalized for a system of N cascaded identical resonators, and a convex optimization problem is formulated for the case where only the coupling between adjacent resonators is considered. To account for the non-adjacent coupling in the system, the solution of the approximating convex optimization is perturbed by performing a second optimization on the full non-convex system using the convex solution as a starting point. This two-step method converges to the global maximum using fast and efficient local optimization algorithms. The convex formulation also provides insights into the optimal spacing of systems containing up to 20 coils transmitting power up to 4.0 m. We apply our spacing optimization to two types of cascaded multi-coil systems composed of identical coils in order to determine (1) the optimal number of coils that maximize efficiency over a fixed distance and (2) the optimal placement of a select number of high-Q coils within a system.

coupling terms are typically much smaller than the direct coupling terms. We should also note that although cross-coupling provides additional paths for power to flow between resonators, these paths do not always increase the power delivered to the load and can introduce impedance mismatches within the system [15].

A general multi-coil system containing N identical coils is considered in this paper, as depicted in Fig. 1. The first coil is connected to the voltage source V_S through a source resistance R_S and the last coil is connected directly to the load R_L. The remaining intermediate coils act like relay coils to transfer power from the source to the load. In order to calculate the power efficiency of the system, we solve for the source-to-load admittance by inverting the system impedance matrix. By normalizing the voltages and currents with respect to the coil resistances R_n, the normalized impedance matrix can be expressed in terms of coupling coefficients, quality factors, and normalized source and load resistances:

$$\begin{bmatrix} V_S/\sqrt{R_1} \\ 0 \\ 0 \\ \vdots \\ 0 \end{bmatrix} = \begin{bmatrix} 1+R_S/R_1 & jk_{12}\sqrt{Q_1Q_2} & jk_{13}\sqrt{Q_1Q_3} & \dots & jk_{1N}\sqrt{Q_1Q_N} \\ jk_{12}\sqrt{Q_1Q_2} & 1 & jk_{23}\sqrt{Q_2Q_3} & \dots & jk_{2N}\sqrt{Q_2Q_N} \\ jk_{13}\sqrt{Q_1Q_3} & jk_{23}\sqrt{Q_2Q_3} & 1 & \dots & jk_{3N}\sqrt{Q_3Q_N} \\ \vdots & \vdots & \vdots & \ddots & \vdots \\ jk_{1N}\sqrt{Q_1Q_N} & jk_{2N}\sqrt{Q_2Q_N} & jk_{3N}\sqrt{Q_3Q_N} & \dots & 1+R_L/R_N \end{bmatrix} \begin{bmatrix} I_1\sqrt{R_1} \\ I_2\sqrt{R_2} \\ I_3\sqrt{R_3} \\ \vdots \\ I_N\sqrt{R_N} \end{bmatrix}. \quad (1)$$

Optimization methodology

We begin our study of multi-coil WPT by deriving the efficiency of a system considering only the direct coupling between coils. This is typically valid when the multi-coil system contains high-quality factor coils with small coupling coefficients between adjacent coils (i.e. when the system contains few coils or transmits power over a large distance). In these systems, the efficiency can be formulated as a convex function, allowing the optimal spacing to be calculated using standard convex optimization methods [18]. Following the formulation of the convex optimization problem, a perturbation is applied to the resulting optimal spacing in order to account for the cross-coupling terms.

System model

A cascaded multi-coil system can be modeled by an equivalent circuit of coupled series RLC resonators [13]. This model allows for accurate calculation of system efficiency through circuit analysis, avoiding the need for computationally expensive full-wave simulations when considering large multi-element systems. Each coil resonates at the operating frequency ω_o and can be modeled by a quality factor Q_n and series resistance R_n (the corresponding inductance and capacitance are then uniquely determined through $\omega_o L_n = 1/\omega_o C_n = R_n Q_n$). The coils are magnetically coupled through mutual inductances represented by the coupling coefficients k_{mn}. These coefficients can be separated into two distinct categories: the direct coupling coefficients between adjacent coils, where $|m-n|=1$, and the cross-coupling coefficients between non-adjacent coils, where $|m-n|\geq 2$. Since the magnetic coupling decays rapidly with distance (approaching an inverse cubed relationship as the distance becomes very large), the higher order

The cross-coupling terms in (1) have been highlighted in grey. When the coils are not tightly coupled and the quality factors are large, these terms can be neglected and the normalized impedance reduces to a tri-diagonal matrix. Solving the matrix equation yields the current at the load, from which the efficiency can be calculated, as shown in the following section.

Convex formulation of system efficiency

The efficiency for the directly coupled system model, η_d, is calculated from the current passing through the load coil, I_N, as determined from the matrix equation in (1). We define the efficiency as the ratio of power delivered to the load over the power available from the source,

$$\begin{aligned} \eta_d &= \frac{P_L}{P_{avs}} = \frac{4R_S R_L |I_N|^2}{|V_S|^2} \\ &= \frac{4\frac{R_S}{(R_S+R_1)}\frac{R_L}{(R_L+R_N)}\prod_{n=1}^{N-1} k_{n,n+1}^2 Q_n' Q_{n+1}'}{\left[K_N(k_{12}^2 Q_1' Q_2', \dots, k_{N-1,N}^2 Q_{N-1}' Q_N')\right]^2}, \end{aligned} \quad (2)$$

where we use the loaded quality factor of each coil

$$\mathbf{Q}' = \begin{bmatrix} Q_1' \\ Q_2' \\ \vdots \\ Q_{N-1}' \\ Q_N' \end{bmatrix} = \begin{bmatrix} Q_1/\left(1+\frac{R_S}{R_1}\right) \\ Q_2 \\ \vdots \\ Q_{N-1} \\ Q_N/\left(1+\frac{R_L}{R_N}\right) \end{bmatrix} \quad (3)$$

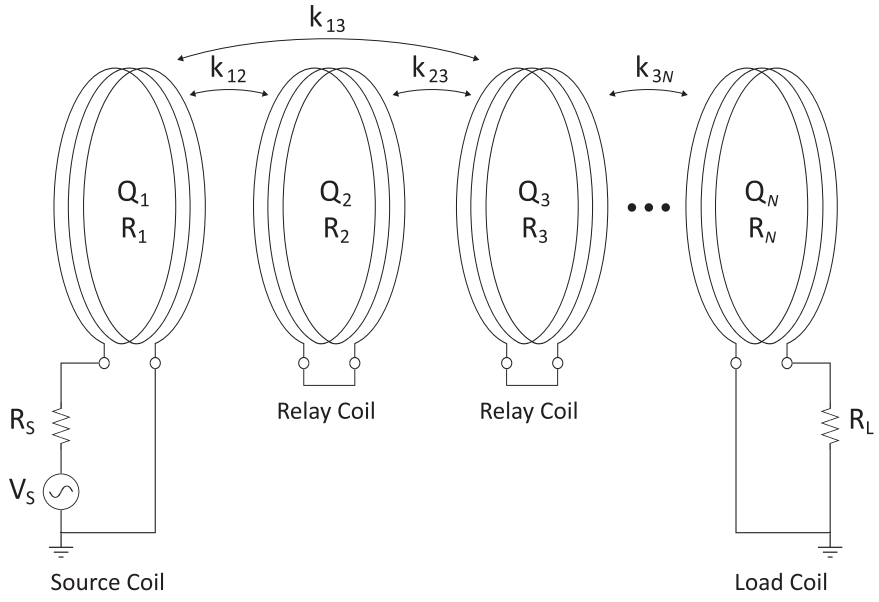

Fig. 1. Equivalent circuit model of a multi-coil WPT system with N coils. Each coil resonates at ω_o with a quality factor Q_n and loss resistance R_n. The source and load coils are connected in series to the source resistance, R_S, and load resistance, R_L, respectively.

in place of Q_n. The function $K_N(a_{12}, \ldots, a_{N-1,N})$ generates a continuant polynomial (representing the determinant of a particular $N \times N$ tri-diagonal matrix) defined through the following recursive relation [19]:

$$\begin{aligned} K_0 &= 1 \\ K_1 &= 1 \\ K_n &= K_{n-1} + a_{n-1,n} K_{n-2}. \end{aligned} \tag{4}$$

These functions are polynomials of $a_{n,n+1}$ with each term containing a positive coefficient.[1]

Our objective in this work is to maximize the efficiency of multi-coil systems. We therefore invert (2) to express it in standard form as a minimization problem:

$$\begin{aligned} \underset{\mathbf{k}}{\text{minimize}} \quad & f_{gp}(\mathbf{k}) = \frac{1}{\eta_d(\mathbf{k}, \mathbf{Q}', R_S/R_1, R_L/R_N)} \\ \text{where} \quad & \mathbf{k} = \left[k_{12}, \ldots, k_{N-1,N} \right]^{\mathrm{T}} \\ \text{subject to} \quad & \mathbf{k} \geq \mathbf{0}, \\ & \mathbf{k} \leq \mathbf{1}. \end{aligned} \tag{5}$$

In (5), $\mathbf{k}$ is the vector of variables to be optimized and contains the direct coupling coefficients. Although the objective function in (5) is not itself convex, it can be recognized as a geometric program f_{gp} with a posynomial numerator and monomial denominator [18]. A geometric program in x_n can be transformed into convex form by substituting new optimization variables $y_n = \ln x_n$ in for x_n. The new objective function becomes an affine function raised to an exponential which is now convex in terms of y_n [18].

[1]For example, the first few polynomials up to $N = 6$ are written as

$$\begin{aligned} K_2 &= 1 + a_{12} \\ K_3 &= 1 + a_{12} + a_{23} \\ K_4 &= 1 + a_{12} + a_{23} + a_{34} + a_{12}a_{34} \\ K_5 &= 1 + a_{12} + a_{23} + a_{34} + a_{45} + a_{12}a_{34} + a_{12}a_{45} + a_{23}a_{45} \\ K_6 &= 1 + a_{12} + a_{23} + a_{34} + a_{45} + a_{56} + a_{12}a_{34} + a_{12}a_{45} \\ &\quad + a_{12}a_{56} + a_{23}a_{45} + a_{23}a_{56} + a_{34}a_{56} + a_{12}a_{34}a_{56}. \end{aligned}$$

Up to this point, the objective function, constraints, and optimization variables have all been expressed in terms of the coupling coefficients. The physical constraints on the system, however, would be more conveniently expressed in terms of distance and spacing. Since the coupling coefficients decrease convexly with increasing distance between coils (as shown by the sample curve in Fig. 2), they can be mapped to coil spacing while maintaining convexity by leveraging the transformation $x_n = \exp(y_n)$ introduced above. Each pair of coils can therefore be approximated locally with the following exponential fit:

$$k(d) \approx f_{n,n+1}(d) = \exp(-\alpha_{n,n+1} d + \beta_{n,n+1}), \tag{6}$$

where $\alpha_{n,n+1}$ and $\beta_{n,n+1}$ are positive exponential fitting parameters relating the coupling coefficients $k_{n,n+1}$ and distance $d_{n,n+1}$ between the n^{th} and $(n+1)^{\text{th}}$ coils. Each set of fitting parameters is calculated such that the values and slopes of $k(d)$ and $f_{n,n+1}(d)$ are matched at $d_{n,n+1}$,

$$f_{n,n+1}(d_{n,n+1}) = k_{n,n+1}, \tag{7}$$

$$\frac{\partial}{\partial d} f_{n,n+1}\Big|_{d_{n,n+1}} = \frac{\partial k}{\partial d}\Big|_{d_{n,n+1}}, \tag{8}$$

as illustrated in Fig. 2. The convex optimization is first performed using default fitting parameters corresponding to equal spacing. Once a set of distances $d_{n,n+1}$ are determined, the $\alpha_{n,n+1}$ and $\beta_{n,n+1}$ coefficients are re-calculated and the optimization is repeated using the solution of the first optimization as a starting point. This iterative procedure converges very quickly, typically requiring only two or three iterations to reach a stable solution.

Now that the optimization objective is formulated as a convex function of coil spacing, we introduce two new convex constraints to the system. First, the total distance, D, is fixed between the source and load coil and set equal to the sum of the spaces in the system. Second, a minimum separation distance between coils, $d_{\min}$, is introduced to prevent physical overlap. Note that

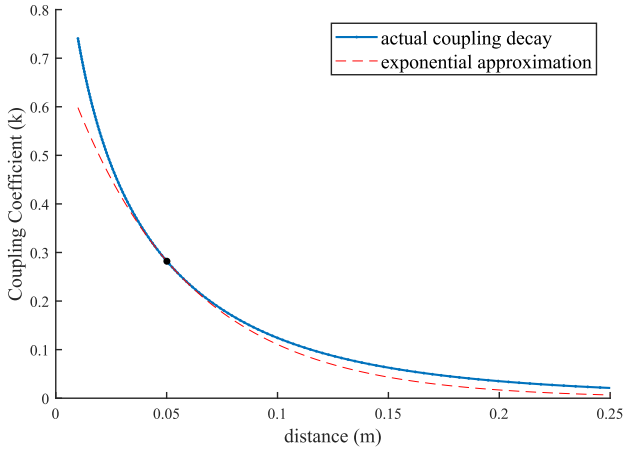

Fig. 2. (Color online) An example of the functional dependence of the magnetic coupling between coils, k, on the distance between them, d, calculated by numerically evaluating the inductance field integrals between conducting loops of major radius 0.1 m and minor radius 0.005 m. The solid blue curve plots the coupling decay as a function of distance, while the dashed red curve plots an exponential function that can be used to locally approximate the coupling at the distance indicated by the black dot.

this minimum distance constraint also ensures the coupling coefficient is always convex with respect to separation distance.

We now summarize the final optimization problem with the convex optimization function f_{cvx} and all constraints below:

$$\begin{aligned} \underset{\mathbf{d}}{\text{minimize}} \quad & f_{cvx}(\mathbf{d}) = \frac{1}{\eta_d(\mathbf{k}, \mathbf{Q}', R_S/R_1, R_L/R_N)} \\ \text{where} \quad & \mathbf{k} = \exp(-\alpha \circ \mathbf{d} + \beta) \\ & \mathbf{d} = \left[d_{12}, \ldots, d_{n,n+1} \right]^T \\ & \alpha = \left[\alpha_{12}, \ldots, \alpha_{n,n+1} \right]^T \\ & \beta = \left[\beta_{12}, \ldots, \beta_{n,n+1} \right]^T \\ \text{subject to} \quad & \mathbf{d} \geq d_{\min}\mathbf{1} \\ & \mathbf{1}^T\mathbf{d} = D, \end{aligned} \tag{9}$$

where $\circ$ is the Hadamard (entrywise) product between vectors.

Cross-coupling perturbation

We have now formulated the efficiency of the multi-coil WPT system as a convex function f_{cvx} of the coil spacing. However, neglecting the higher order cross-coupling terms decreases the accuracy of the optimal spacing values for maximum efficiency. It also limits the ability to optimize systems in which the cross-coupling significantly impacts the efficiency. Examples of these systems include tightly packed coils within short transmission distances and large systems with low-quality factor coils. An optimization procedure which accounts for the cross-coupling terms must therefore be developed to ensure the convex formulation is useful for applications requiring high precision.

By including the cross-coupling terms in our system model, the equation for efficiency is no longer convex, and thus convex optimization cannot be directly applied. However, because the cross-coupling terms are typically much smaller than the direct coupling terms, we can treat them as perturbations to the convex system model. Thus, an additional step can be applied to the optimization process to account for this perturbation to the convex optimal efficiency solution. The first step in the overall optimization procedure is to apply the convex optimization to the direct coupling model, as presented in the previous section. The optimal spacing values from this first step are then used as the starting point of an efficiency optimization based on the complete coupling matrix from (1). In both steps, a non-linear programming solver based on an interior point algorithm is used [20]. The second step perturbs the convex solution by converging to the nearest optimum of the non-convex system. By feeding the solver a starting point determined from the optimal solution of the approximating convex system, the results from the second step of the optimization converge quickly to the global optimum. The assumption underlying this perturbation model is that the approximating convex solution is closer to the global optimum of the cross-coupled system than any other local optimum, which is valid in the limit as cross-coupling goes to zero.

Comparison of convex and perturbed convex optimization

A comparison can now be made between the spacing results of the convex optimization and the perturbed convex optimization. First, the optimal spacing configurations which maximize the system efficiency are determined for the convex model. Next, the optimal spacing of the system is determined from the two-step optimization, and the results are compared. Finally, the accuracy of the convex model is evaluated by comparing the solutions from the convex optimization to full-wave simulations and to the solutions of an independent quasi-global optimization method.

In our study, we consider WPT systems composed of 4–20 coils operating over distances ranging from 0.3 to 4.0 m, with each coil having a quality factor of 150. Each coil is modeled as a conducting loop (i.e. a torus) with a 1 cm minor diameter and a 20 cm major diameter. The self and mutual inductances of the coils were calculated by numerically evaluating the inductance field integrals [21] and corroborated by full-wave simulations using an in-house full-wave solver based on the Multiradius Bridge Current (MBC) moment method [22]. These inductances were then used to calculate the mapping between coupling coefficient and distance discussed in the previous section (plotted in Fig. 2). The capacitance of the coils was chosen to ensure resonance at 13.56 MHz, while the coil resistance was chosen to specify one of the three quality factors considered in our study: $Q = 50$, $Q = 150$, and $Q = 350$. These resistance values include ohmic losses, capacitor losses, and radiation losses, the latter being on the order of $10^{-4}\,\Omega$ for loops of radius 0.1 m at 13.56 MHz [23]. The width of the loop introduces an additional constraint on the spacing of the system, limiting the center-to-center distance between coils to $d_{\min} = 1$ cm. We assume the chain of resonators will be connected to a 50 Ω system and set our source and load impedances equal to this value ($R_S = R_L = 50\,\Omega$). A complete list of model parameters is provided in Table 1.

Convex optimization

Figure 3 depicts the optimal spacing of various multi-coil systems at a transmission distance of 0.6 m, with Fig. 3(a) illustrating the position of the spaces between coils. In Fig. 3(b), we observe a characteristic non-uniform spacing pattern consisting of short gaps at each end of the coil system, followed by transition gaps into the quasi-uniform spacing between the 3rd and 3rd-to-last coils. The short separation distance between the low-Q loaded

Table 1. Parameter values for the *N*-coil cascaded resonator systems studied in sections "Comparison of convex and perturbed convex optimization" and "Cascaded multi-coil optimization studies"

Element name(s)	Element value	Units
R_n	0.648 for $Q = 50$	Ω
	0.216 for $Q = 150$	
	0.0925 for $Q = 350$	
L_n	0.380	μH
C_n	0.363	nF
R_S, R_L	50	Ω
f_o	13.56	MHz
Loop major radius	0.1	m
Loop minor radius	0.005	m

source coil and the first relay coil enables power to be transferred into the cascaded coil system without the need for large source currents. The adjacent transition gap then provides the impedance transformation that matches the source coil to the uniformly spaced cascaded interior relays. This spacing is then reversed at the load end of the system to couple power from the relays back to the load. The use of tightly spaced high-Q coils adjacent to the source and load coil systems as a method of impedance transformation and improved power transfer efficiency is commonly seen in four-coil MRC WPT systems [24]. By extending the optimization of these systems to increasing numbers of coils, it is seen that this characteristic spacing is present all the way through to systems containing 20 coils. Note that although only a 0.6 m system is shown here, this spacing profile is present in systems operating over all transmission distances.

Non-uniform end spacing has been observed in systems of up to eight coils [10, 15], but the suggested explanation that it is due to the end coils being adjacent to only one other coil does not sufficiently explain the characteristic spacing observed in larger systems. The quasi-uniform spacing away from the ends of the chain implies that the source and load impedances are being matched to the impedance of the interior cascaded relay coils. This cascaded relay impedance can be calculated by considering the image impedance of an infinite periodic chain of identical resonators. Using the equation for the effective impedance of each coil [24], the image impedance at the coil resonance frequency is purely real and given by

$$R_{\text{image}} = R + \frac{\omega^2 k^2 L^2}{R + R_{\text{image}}} = R + \frac{R^2 k^2 Q^2}{R + R_{\text{image}}}, \tag{10}$$

where k is the coupling coefficient between adjacent resonators, and R, L, and Q are the resistance, inductance, and quality factor of each resonator, respectively. R_{image} can be solved for as

$$R_{\text{image}} = \sqrt{R^2 + \omega^2 k^2 L^2} = R\sqrt{1 + k^2 Q^2}. \tag{11}$$

Since R and kQ are typically not large, the image resistance of a system of chained resonators is typically much lower than 50 Ω. The image resistance increases with tighter spacing (larger k) and decreases with relaxed spacing (smaller k). For example, the image resistance can be calculated at the center of the 20-coil system in Fig. 3(b). The frequency, inductance, and resistance of the

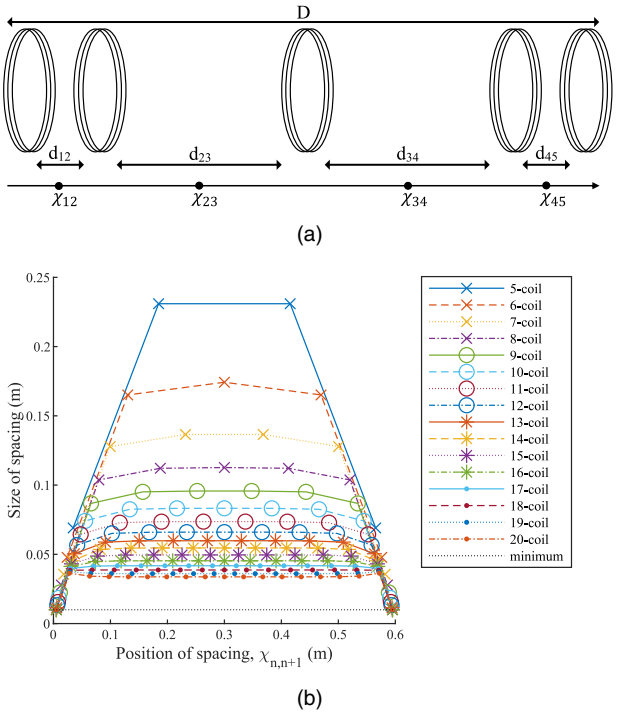

Fig. 3. (Color online) (a) A sample model of a five-coil WPT system with a total transmission distance, D, and individual coil spaces, $d_{n,n+1}$. The midpoint between each pair of coils is marked on the horizontal line below the coils to provide a reference position for the space between each pair of coils. These positions can be expressed in terms of the distances as $\chi_{n,n+1} = 0.5\, d_{n,n+1} + \sum_{i=1}^{n-1} d_{i,i+1}$. (b) The optimal spacing for multi-coil systems at a transmission distance of 0.6 m assuming direct coupling only. The black dotted line indicates the minimum spacing constraint used in the optimization.

coils are known, and the coupling coefficient k can be determined from the center spacing. Using (11), the image resistance over the inner 16 coils of the chain is approximately 8.4 Ω. In order to match the source and load coil impedance to this low image impedance, the 2nd and 2nd-to-last gaps increase to provide the appropriate inductive transformation to 50 Ω.

Perturbed convex optimization

As outlined in section "Optimization methodology", the perturbed convex optimization can be performed by optimizing the fully cross-coupled system using the spacing from the convex optimization as a starting point. Figures 4 and 5 depict the optimal spacing of a system with $Q = 150$ at a transmission distance of 0.6 m using this two-step optimization. As can be seen in Fig. 4, the largest spaces between coils occur near the center of the chain for systems with low N. As the number of coils in the system increases, the spacing between all internal coils becomes more uniform. For systems with larger values of N, the position of the largest spaces changes to lie between the 2nd and 3rd coils from each end of the system, as visible in the 20-coil system in Fig. 4. This transition is consistent with the observations of the characteristic spacing made from the direct coupling optimized system in section "Convex optimization". The most notable difference from the optimal spacing of the convex approximation in Fig. 3(b) is the light clustering of coils along the resonator chain.

Figure 5 compares the spacing results from the convex optimization (solid-line) with the spacing results from the perturbed convex optimization (dashed-line). At a distance of 0.6 m, it is seen that

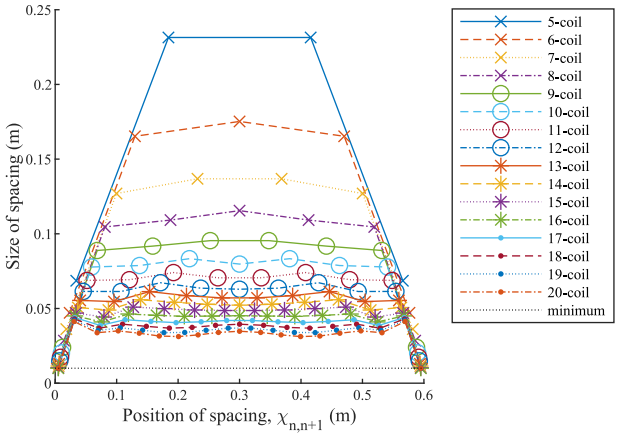

Fig. 4. (Color online) Optimal spacing from the perturbed convex optimization for an $N = 5$ to $N = 20$ coil system at a transmission distance of 0.6 m.

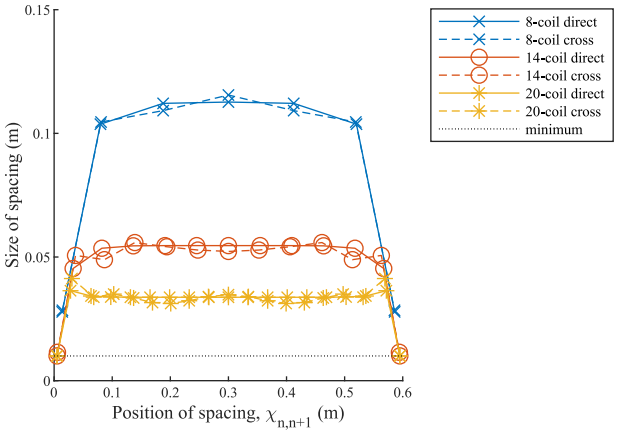

Fig. 5. (Color online) Optimal spacing for an $N = 8$, $N = 14$, and an $N = 20$ coil system at a transmission distance of 0.6 m. The direct coupling optimized results are displayed with solid lines, while the cross-coupling full optimization results are displayed with dashed lines.

systems with nine or fewer coils have optimal spacing configurations in close agreement. However, in systems with $N \geq 10$, as observed with the 14- and 20-coil systems in Fig. 5, the coils optimized using the perturbed convex model begin to form light clusters. This is clearly visible in Fig. 5, with the 20-coil system containing denser packing at the 0.2 and 0.4 m positions. While there are deviations between the two optimization results for systems with more coils, it can be seen that the trend of tightly-packed end coils and moderately-spaced relay coils is present in both optimizations. That is, the characteristic spacing of an optimized chain of cascaded multi-coil WPT is observable from both the convex optimization and the perturbed convex optimization.

Accuracy of the convex model

To determine the limitations of the convex model on accurately representing cascaded multi-coil systems, we compare the efficiency determined by the convex and perturbed convex (two-step) optimizations. We then compare the calculated efficiencies from the equivalent circuit model to the efficiencies simulated using MBC, our full-wave moment method solver. All three efficiencies are compared in Fig. 6(a) for cascaded WPT systems of up to 20 coils over four transmission distances. The convex optimization efficiency as formulated in section "Convex formulation of system efficiency" is plotted with circle markers, the perturbed convex optimization efficiency as formulated in section "Cross-coupling perturbation" is plotted with cross-markers, and the efficiency determined by MBC is plotted with plus markers.

In Fig. 6(b), we plot the efficiency curves from the perturbed convex optimization alongside the efficiency curves generated from a much slower quasi-global optimization method. A genetic algorithm (GA) was chosen with a population of 250 optimized over 2500 generations. The efficiency from the perturbed convex optimization never fell below the result from the GA, verifying that our method appears to converge to the global optimum. A discrepancy of up to 2% can be observed between optimization solutions, with the GA efficiency curves lacking the smoothness of the perturbed convex optimization curves. We have verified that applying a local optimization as a second step following the completion of the GA (not shown) does result in the exact solution of the perturbed convex method.

It is clear from these figures that formulating the efficiency of cascaded multi-coil WPT systems as a convex function of spacing allows for reliable optimization. Firstly, by comparing the efficiency results of the convex model and the perturbed convex model in Fig. 6(a), it is seen that the optimal efficiencies are within 1.0% for systems with up to 20 coils packed into 30 cm. The maximum spacing error of the convex optimization with respect to the perturbed convex optimization is quantified in Fig. 6(c) as a percent of the total transmission distance. Overall, the convex optimization yields a spacing which only deviates from the optimal spacing of the fully cross-coupled system by 2.5% at a transmission distance of 30 cm, and for more loosely spaced systems (such as the 90 and 120 cm transmission distances), this deviation remains below 0.7%. Secondly, by comparing the perturbed convex solution to the simulated efficiencies in Fig. 6(a), we see that they agree to within 0.5% of each other. This validates the accuracy of the equivalent circuit model and demonstrates the effectiveness of the perturbed convex optimization in providing an optimal coil spacing. Thirdly, since the perturbed convex solution is always greater than or equal to the GA solution plotted in Fig. 6(b), the quasi-global nature of the method is validated.

Cascaded multi-coil optimization studies

Using the two-step perturbed convex optimization technique presented in the section "Cross-coupling perturbation", we now maximize the efficiency of large multi-coil systems. In this section, the perturbed convex optimization is applied to two types of WPT systems containing up to 20 coils. The first study focuses on the change in efficiency as the number of coils increases over a fixed distance. The second study considers the optimal spacing for systems containing coils with a combination of high- and low-quality factor coils.

Optimal N for a fixed distance

The first study compares systems of N identical resonators over various transmission distances. Three different types of systems are considered: one with $Q = 50$ coils, one with $Q = 150$ coils, and one with $Q = 350$ coils. The peak achievable efficiencies of these systems can then be directly compared to view the impact of Q on efficiency. At each transmission distance, the number of coils in the system is swept from 4 to 20. Comparing the efficiency achieved by each system at a given distance allows for an optimal number of coils to be determined.

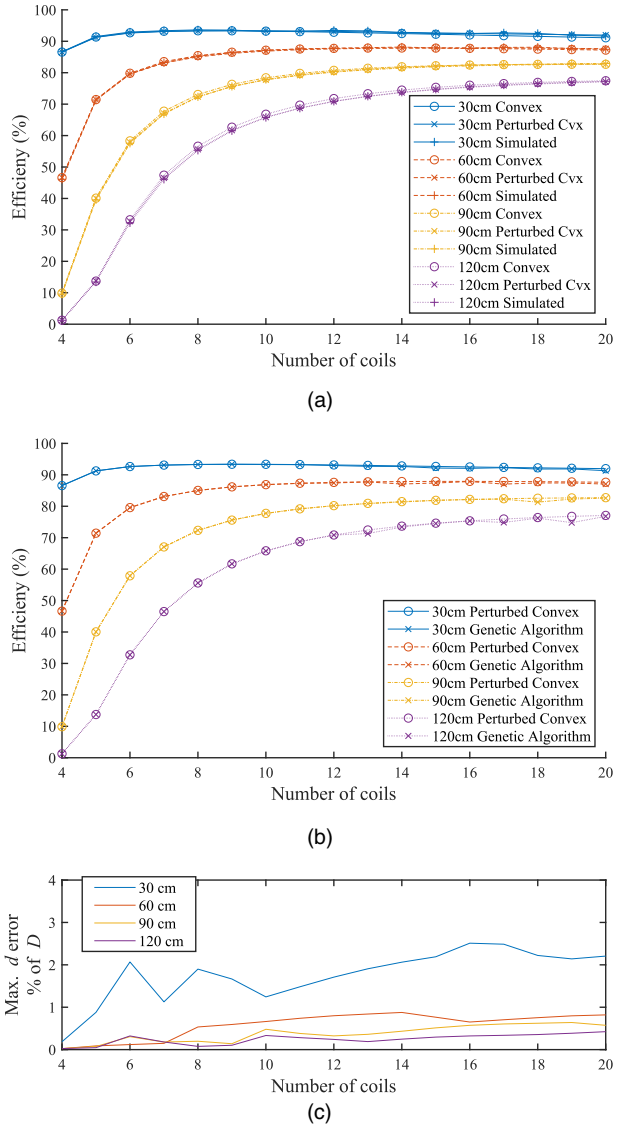

Fig. 6. (Color online) (a) Optimal efficiency from the direct coupling convex model (circle markers), the optimal efficiency from the perturbed convex model (cross-markers), and the simulated efficiency from the MBC solver using the optimal spacing of the perturbed convex system (plus markers) for transmission distances of 0.3–1.2 m. The convex solution and the perturbed convex solution agree within 1.0%. (b) Optimal efficiency from the perturbed convex model (circle markers), the optimal efficiency from a quasi-global genetic algorithm with a population of 250 over 2500 generations (cross-markers) for transmission distances from 0.3 to 1.2 m. (c) The maximum spacing error of the convex optimization solution from the perturbed convex solution, as a percent of the total transmission distance.

Figure 7 illustrates the peak achievable efficiency for transmission distances from 0.3 to 1.0 m for systems with (a) $Q = 50$, (b) $Q = 150$, and (c) $Q = 350$. The quality factors of these systems were modified by changing the losses of the coils through R_n (see Table 1 for a list of all parameters used). We can see from the figure that the efficiency of a four-coil WPT system can be significantly improved by adding relay coils between the source and load. Efficiency is improved for all cascaded resonator systems tested, regardless of quality factor. That being said, we do observe an interesting feature in the efficiency response as more coils are placed in the system. The efficiency does not increase monotonically with an increasing number of coils. Instead, it increases to a peak value, before slowly beginning to decrease with the addition of each subsequent coil. It turns out that the drop in efficiency with increasing N is a consequence of using coils with identical loading as well as the requirement that the coils be matched to a fixed system impedance. For example, consider

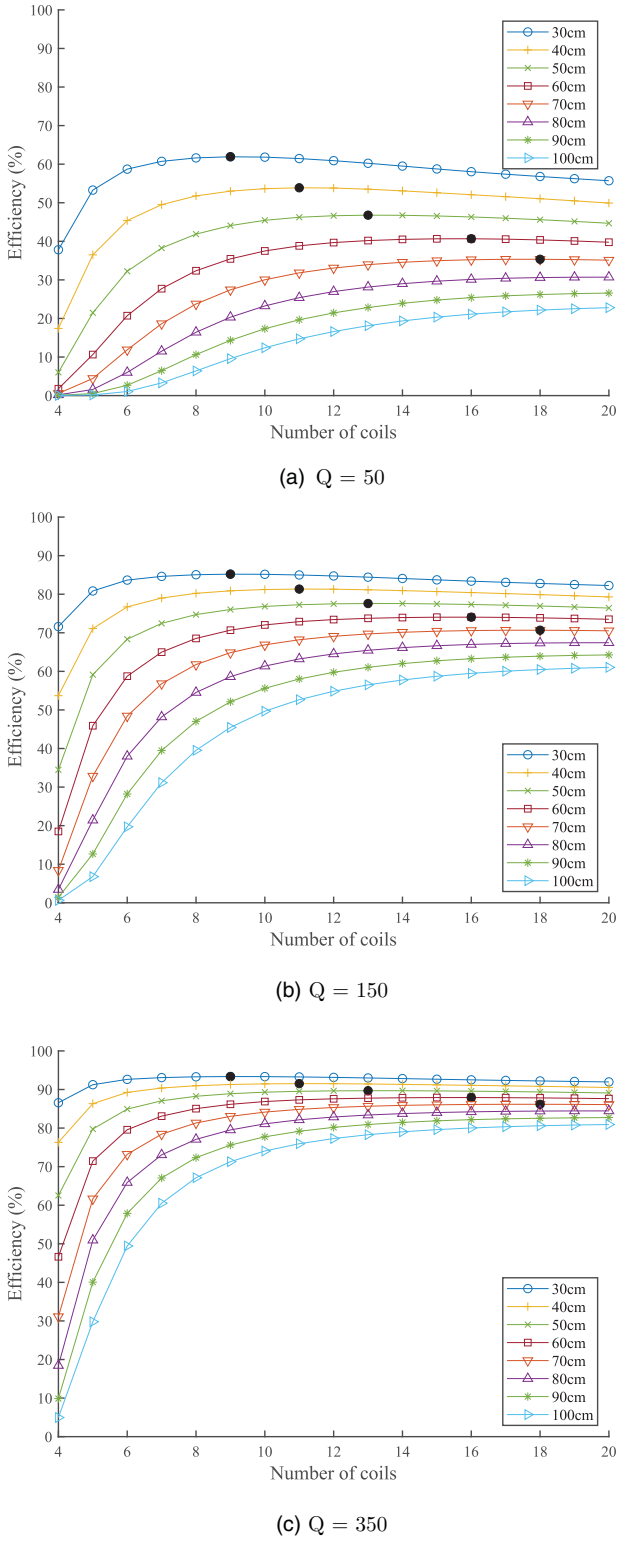

Fig. 7. (Color online) Optimal system efficiency as a function of an increasing number of coils over transmission distances from 0.3 to 1.0 m. The systems contain coils with quality factor (a) $Q = 50$, (b) $Q = 150$, and (c) $Q = 350$. The maximum efficiency for a fixed distance is marked with a solid black circle.

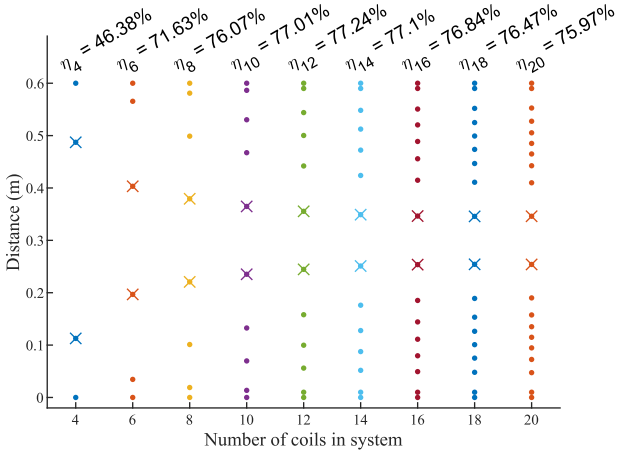

Fig. 8. (Color online) Optimal efficiency and spacing of multi-coil systems containing two high-Q coils and transmitting power over a distance of 60 cm. The optimal $Q = 350$ coil placements are indicated by an "x", while the optimal placements of the remaining $Q = 150$ coils are indicated with dots. The efficiency of each system is displayed above its respective position diagram.

that as the number of coils increases, the average spacing between coils decreases. This increases the coupling between coil pairs for a higher potential power transfer rate; however, it also degrades the impedance transformation at the source and load. When the number of coils is low, each additional coil improves the efficiency by increasing the coupling between coils. Once the number of coils surpasses the optimal number, however, the additional mismatch at the source and load outweigh the tighter coupling between relay coils and the efficiency begins to drop.

In each plot in Fig. 7, the system with peak efficiency for a given transmission distance is indicated by a solid black circle. For example, the $Q = 150$ system (Fig. 7(b)) achieves a peak efficiency with nine coils when transmitting power over a distance of 30 cm, while at 40 cm, this peak occurs with 11 coils. Note that the optimal number of coils is mostly independent of the quality factor, appearing at the same positions for all three quality factors. For the systems with lower coil counts (i.e. $N = 4, 5, 6$), a large increase in efficiency can be observed from including a single additional coil to the system. Beyond this, each additional coil produces a decreasing marginal improvement. It is therefore worthwhile to note that a six-coil system sufficiently outperforms many of the four-coil systems and might provide a practical compromise between system complexity and efficiency. For example, by adding two relay coils to the four-coil, $Q = 150$ system at 40 cm, efficiency can be improved by 23.0%, whereas the four additional coils needed to reach the optimal 11-coil configuration only improve the efficiency by another 4.6%.

Optimal placement of high-Q coils

In this section, we investigate the capability of the perturbed convex optimization method to determine the optimal spacing and the optimal placement of resonators when coils of various quality factor are used. In this experiment, we characterize a system containing two high-Q coils with $Q = 350$ within a cascaded chain of low-Q coils with $Q = 150$. By substituting a select number of high-Q coils into the system, one can improve the efficiency of the system without incurring the cost of replacing every coil in the system with high-Q coils.

To investigate the optimal placement of high-Q coils, we introduce an outer loop into the optimization which moves the high-Q coils through every possible combination of positions in the system, and selects the peak efficiency from across those permutations. Because of the convex optimization's robustness and speed, these optimizations can be performed quickly and efficiently. The optimal coil placements and efficiencies are plotted in Fig. 8 for systems spanning a distance of 60 cm. For five of the nine systems presented, the optimal efficiency occurs when the high-Q coils are placed in the middle of each relay chain on either side of the large central gap. In the remaining four systems, the high-Q coils bookend the largest gap as it moves away from the center position. In all configurations, the optimal positions of the high-Q coils are adjacent to each other. This placement is consistent with our understanding of MRC power transfer, where the largest spaces between coils correspond to the smallest coupling coefficients and act like bottlenecks to limit the power transfer. Placing high-Q coils on either side of these spaces enables large resonant currents that generate strong magnetic fields to couple power across the gap. This placement mitigates the largest drop in power along the relay chain and therefore provides the greatest improvement to the efficiency of the system.

The benefits to the efficiency with the addition of just two high-Q coils is illustrated by comparing the efficiencies of the six-coil systems in Figs 7 and 8 for a transmission distance of 60 cm. Replacing two of the $Q = 150$ coils with $Q = 350$ coils boosts the efficiency by 12.9%, compared with a 20.8% improvement from replacing all six coils in the system. These results illustrate the effectiveness of perturbed convex optimization in determining the optimal spacing of cascaded multi-coil WPT systems and determining the optimal spacing with resonators of different Q factors.

Conclusion

In this paper, we applied convex optimization to the design of maximum-efficiency cascaded multi-coil WPT systems by optimizing the spacing of a chain of identical relay coils. We showed that the efficiency of a multi-coil system can be formulated as a convex function provided that the coupling between coils is assumed to be between adjacent coils only. The cross-coupling terms can then be modeled as a perturbation to the directly-coupled system by performing a local optimization of the cross-coupled system using the solution of the convex optimization as a starting point. This two-step optimization converges to the global optimum when the cross-coupling terms are small and the convex solution is local to the global optimum. By comparing this perturbed convex solution to the results of a full-wave simulation as well as to the solution from a quasi-global genetic optimization, we show that the convex solution provides a very good approximation to the fully cross-coupled solution and that the perturbed convex formulation is a reliable method for ensuring convergence to the global optimum.

We then apply the convex optimization to systems of identical relay coils and show that when spacing alone is optimized, there exist an optimal number of coils to maximize efficiency. This optimal number is dependent on the transmission distance and the quality factor of the coils. From a practical standpoint, adding two or three relay coils to a four-coil system tended to provide the highest efficiency gains per added coil, with gains of around 25%. Finally, we showed that the convex optimization can provide a foundation for the optimization of other system parameters, such as determining the optimal placement of a select number of high-Q coils within a larger system.

In summary, we used convex optimization to design maximum efficiency cascaded multi-coil systems and used our results to present practical design strategies. These findings can be used to select the number of coils and locations of select high-Q coils in multi-coil systems assembled from a set of identical resonators. Furthermore, this work provides insights into the relationship between coupling and spacing in cross-coupled systems, and provides a detailed analysis of the characteristic spacing seen in optimized systems. Optimally spaced systems can be implemented using identical resonators and therefore provide a practical alternative to loading relay coils with individualized reactances.

Acknowledgements. The authors acknowledge CMC Microsystems for the provision of CAD tools that facilitated this research.

Financial support. This work was supported by the Natural Sciences and Engineering Research Council of Canada (NSERC RGPIN-2014-03639). Infrastructure was purchased through the Canada Foundation for Innovation and the British Columbia Knowledge Development Fund (CFI JELF 34805).

Conflict of interest. None.

References

[1] **Park J, Kim D, Hwang K, Park HH, Kwak SI, Kwon JH and Ahn S** (2017) A resonant reactive shielding for planar wireless power transfer system in smartphone application. *IEEE Transactions on Electromagnetic Compatibility* **59**, 695–703.

[2] **Yang Y, El Baghdadi M, Lan Y, Benomar Y, Van Mierlo J and Hegazy O** (2018) Design methodology, modeling, and comparative study of wireless power transfer systems for electric vehicles. *Energies* **11**, 1716.

[3] **Reza Khan S and Choi G** (2016) Optimization of planar strongly coupled wireless power transfer system for biomedical applications. *Microwave and Optical Technology Letters* **58**, 1861–1866.

[4] **Huang C, Kawajiri T and Ishikuro H** (2018) A 13.56-mhz wireless power transfer system with enhanced load-transient response and efficiency by fully integrated wireless constant-idle-time control for biomedical implants. *IEEE Journal of Solid-State Circuits* **53**, 538–551.

[5] **Kurs A, Karalis A, Moffatt R, Joannopoulos JD, Fisher P and Soljačić M** (2007) Wireless power transfer via strongly coupled magnetic resonances. *Science* **317**, 83–86.

[6] **Imura T and Hori Y** (2017) Unified theory of electromagnetic induction and magnetic resonant coupling. *Electrical Engineering in Japan* **199**, 58–80.

[7] **Mi CC, Buja G, Choi SY and Rim CT** (2016) Modern advances in wireless power transfer systems for roadway powered electric vehicles. *IEEE Transactions on Industrial Electronics* **63**, 6533–6545.

[8] **Lee K, Pantic Z and Lukic SM** (2014) Reflexive field containment in dynamic inductive power transfer systems. *IEEE Transactions on Power Electronics* **29**, 4592–4602.

[9] **Zhang Y, Lu T, Zhao Z, Chen K, He F and Yuan L** (2015) Wireless power transfer to multiple loads over various distances using relay resonators. *IEEE Microwave and Wireless Components Letters* **25**, 337–339.

[10] **Zhong W, Lee CK and Hui SR** (2013) General analysis on the use of tesla's resonators in domino forms for wireless power transfer. *IEEE Transactions on Industrial Electronics* **60**, 261–270.

[11] **Zhang X, Ho S and Fu W** (2012) Quantitative design and analysis of relay resonators in wireless power transfer system. *IEEE Transactions on Magnetics* **48**, 4026–4029.

[12] **Zhang F, Hackworth SA, Fu W, Li C, Mao Z and Sun M** (2011) Relay effect of wireless power transfer using strongly coupled magnetic resonances. *IEEE Transactions on Magnetics* **47**, 1478–1481.

[13] **Zhong WX, Lee CK and Hui S** (2012) Wireless power domino-resonator systems with noncoaxial axes and circular structures. *IEEE Transactions on Power Electronics* **27**, 4750–4762.

[14] **Lee K and Chae SH** (2018) Power transfer efficiency analysis of intermediate-resonator for wireless power transfer. *IEEE Transactions on Power Electronics* **33**, 2484–2493.

[15] **Lee CK, Zhong WX and Hui SYR** (2012) Effects of magnetic coupling of nonadjacent resonators on wireless power domino-resonator systems. *IEEE Transactions on Power Electronics* **27**, 1905–1916.

[16] **Lang HD, Ludwig A and Sarris CD** (2014) Convex optimization of wireless power transfer systems with multiple transmitters. *IEEE Transactions on Antennas and Propagation* **62**, 4623–4636.

[17] **Lang HD and Sarris CD** (2017) Optimization of wireless power transfer systems enhanced by passive elements and metasurfaces. *IEEE Transactions on Antennas and Propagation* **65**, 5462–5474.

[18] **Boyd SP and Vandenberghe L** (2004) *Convex Optimization*. Cambridge, UK: Cambridge University Press.

[19] **Muir T** (1882) *A Treatise on the Theory of Determinants: With Graduated Sets of Exercises for Use in Colleges and Schools*. London, UK: MacMillan and Co.

[20] **Byrd RH, Hribar ME and Nocedal J** (1999) An interior point algorithm for large-scale nonlinear programming. *SIAM Journal on Optimization* **9**, 877–900.

[21] **Jackson JD** (1999) *Classical Electrodynamics*, 3rd Edn, Hoboken, NJ: John Wiley and Sons, Inc.

[22] **Tilston MA and Balmain KG** (1990) A multiradius, reciprocal implementation of the thin-wire moment method. *IEEE Transactions on Antennas and Propagation* **38**, 1636–1644.

[23] **Balanis CA** (2016) *Antenna Theory: Analysis and Design*. New Jersey, US: John Wiley & sons.

[24] **Badowich C and Markley L** (2018) Idle power loss suppression in magnetic resonance coupling wireless power transfer. *IEEE Transactions on Industrial Electronics* **65**, 8605–8612.

Connor Badowich obtained his B.A.Sc. and M.A.Sc. degrees in electrical engineering from the University of British Columbia (UBC), Kelowna, BC, Canada in 2016 and 2019, respectively. While completing his Master of Applied Science degree he worked as a graduate research assistant in the applied electromagnetics laboratory at UBC under the supervision of Dr. Markley. He is currently working in the aerospace industry and continues to collaborate with Dr. Markley. His research interests are in the field of electromagnetics, microwave engineering, and wireless power transfer.

Jacques Rousseau received the B.A.Sc. degree in electrical engineering from the University of British Columbia, Kelowna, Canada, in 2019. As an undergraduate, he was involved in research on wireless power transfer and electronic gas sensor development.

Loïc Markley received the B.A.Sc. degree in electronics engineering from Simon Fraser University, BC, Canada, in 2004, and the M.A.Sc. and Ph.D. degrees in electrical engineering from the University of Toronto, ON, Canada, in 2007 and 2013, respectively. He is currently an Assistant Professor in the School of Engineering at the University of British Columbia, Kelowna, BC, Canada. His research interests include applied electromagnetics, periodic structures and metamaterials, subwavelength imaging, frequency-selective surfaces, leaky-wave antennas, wireless sensing, and wireless power transfer. Since 2015, Prof. Markley has served as Associate Editor for IEEE Antennas and Wireless Propagation Letters. In 2010 he was the recipient of the Tatsuo Itoh Best Paper Award for his paper on near-field focusing published in *IEEE Microwave and Wireless Components Letters*.